Heterodinuclear Bis(diphenylphosphino)methane-Bridged Molybdenum(d^6)-Palladium(d^8) Complexes with Dative Mo→Pd Bonding

Alan L. Balch,* Bruce C. Noll, Marilyn M. Olmstead, and Dawn V. Toronto

Department of Chemistry, University of California, Davis, California 95616

Received March 17, 1993

Investigation of the reaction between $(t\text{-BuNC})_2PdCl_2$ and *mer*-Mo(dpm-*P,P'*)(dpm-*P*)$(CO)_3$ (dpm = bis(diphenylphosphino)methane) has produced two complexes that combine a d^6 and a d^8 metal center. The reaction in dichloromethane yields green $[(t\text{-BuNC})(OC)_3Mo(\mu\text{-dpm})_2PdCl]Cl$ (**6**). Addition of 1 equiv of $[(n\text{-Bu})_3(n\text{-Pr})N]I$ and ammonium hexafluorophosphate to $[(t\text{-BuNC})(OC)_3Mo(\mu\text{-dpm})_2PdCl]Cl$ (**6**) yields golden brown $[(t\text{-BuNC})(OC)_3Mo(\mu\text{-dpm})_2PdI](PF_6)$ (**7**). Orange-brown plates of $[(t\text{-BuNC})(OC)_3Mo(\mu\text{-dpm})_2PdI](PF_6)\cdot 0.5Et_2O\cdot H_2O$ form in the tetragonal space group $I\bar{4}2m$ with a = 22.822(4) Å and c = 27.013(7) Å at 130 K with Z = 8. Refinement of 3764 reflections and 388 parameters yielded R = 0.049 and R_w = 0.053. The structure consists of a seven-coordinate molybdenum atom with a nearly octahedral *trans*-$P_2Mo(CO)_3(CNBu\text{-}t)$ core that is connected to a $(P_2PdI)^+$ unit through the two dpm bridges. The Mo–Pd bond length is 2.870(2) Å. Reaction of $(t\text{-BuNC})_2PdCl_2$ and *mer*-Mo(dpm-*P,P'*)(dpm-*P*)$(CO)_3$ in benzene yields dark brown crystals of $(t\text{-BuNC})(OC)ClMo(\mu\text{-CO})(\mu\text{-dpm})_2PdCl$ (**8**). Red-brown blocks of $(t\text{-BuNC})(OC)ClMo(\mu\text{-CO})(\mu\text{-dpm})_2PdCl\cdot 2CHCl_3$ form in the monoclinic space group $P2_1/c$ with a = 11.825(6) Å, b = 21.508(12) Å, c = 24.441(13) Å, and β = 100.77(4)° at 130 K with Z = 4. Refinement of 6413 reflections and 329 parameters yielded R = 0.069 and R_w = 0.061. This structure parallels the former with the exceptions that the terminal ligand bound to palladium is now a chloride ligand and one of the carbon monoxide ligands on molybdenum has been replaced by a terminal chloride ligand. The Mo–Pd bond length is 2.826(2) Å. The structure of the previously reported $(OC)_3(NC)Mo(\mu\text{-dpm})_2Pd(CN)$ has also been examined. $(OC)_3(NC)Mo(\mu\text{-dpm})_2Pd(CN)\cdot CH_3OH\cdot 0.5H_2O$ crystallizes in the triclinic space group $P\bar{1}$ with a = 12.486(3) Å, b = 15.213(6) Å, c = 16.511(7) Å, α = 116.85(2)°, β = 96.17(2)°, and γ = 95.40(2)° at 130 K with Z = 2. Refinement of 4918 reflections and 268 parameters yielded R = 0.083 and R_w = 0.089. The structure consists of a *trans*-$Mo(\mu\text{-dpm})_2Pd$ core with three terminal carbonyl groups and a cyanide ligand bound to molybdenum and a terminal cyanide ligand attached to palladium. The Mo–Pd distance is 2.926(2) Å.

Introduction

The ditertiary phosphine bis(diphenylphosphino)methane, dpm, has been widely used as a bridging ligand that can position metal ions close together.[1-3] A number of studies from this laboratory have been concerned with the nature of metal–metal interactions within the uniform framework of the dibridged *trans*-$M(\mu\text{-dpm})_2M'$ unit.[1] This unit has considerable flexibility which allows it to accommodate a wide range of M–M' bonding situations and distances. Thus in $Mo_2(\mu\text{-dpm})_2Cl_4$, the Mo–Mo quadruple bond shortens the M–M separation to 2.138(2) Å,[4] while in $Os_2(\mu\text{-}O)(\mu\text{-dpm})_2Cl_6$, the Os–Os separation is 3.584(1) Å and a linear μ-oxo bridge separates the two metal centers.[5]

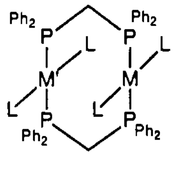

1

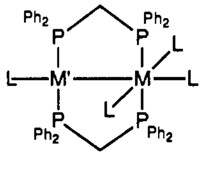

2

Recent work has focused on the effects of asymmetry within the $M(\mu\text{-dpm})_2M'$ unit. The existence of two types of d^8/d^8 complexes, the face-to-face or 4:4 compounds **1** and the less common, less symmetrical 3:5 arrangement **2**, has been demonstrated.[6,7] Other work has shown that significant bond shortening accompanies the addition of an axial ligand to the highly luminescent d^8/d^{10} complex **3** (eq 1).[8] In attempts to extend such studies to include the more sterically crowded d^6 metal centers, it was found that the d^6/d^{10} molybdenum/gold complex **5** existed with an essentially repulsive interaction between the two metal ions.[9]

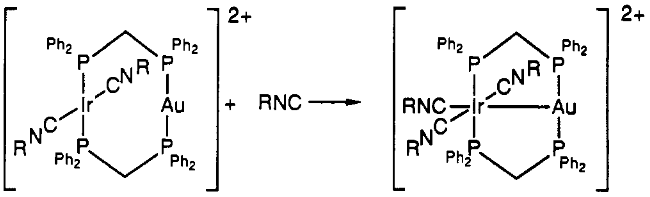

3
Ir-Au, 2.944 Å

4
Ir-Au, 2.817 Å

(1)

Here we report the preparation and structural characterization of a set of heterobinuclear d^6/d^8 molybdenum(0)/palladium(II) complexes that allow interesting comparisons with **5**. For part of this work we examined the reactions of *mer*-Mo(dpm-*P,P'*)-

---

(1) Balch, A. L. In *Homogeneous Catalysis with Metal Phosphine Complexes*; Pignolet, L. H., Ed.; Plenum Press: New York, 1983; p 167.

(2) Puddephatt, R. J. *Chem. Soc. Rev.* **1983**, 99.

(3) Chaudret, B.; Delavaux, B.; Poilblanc, R. *Coord. Chem. Rev.* **1988**, *86*, 191.

(4) Abbott, E. H.; Bose, K. S.; Cotton, F. A.; Hall, W. T.; Sekutowski, J. C. *Inorg. Chem.* **1978**, *17*, 3240.

(5) Chakravarty, A. R.; Cotton, F. A.; Schwotzer, W. *Inorg. Chem.* **1984**, *23*, 99.

(6) Balch, A. L.; Catalano, V. J. *Inorg. Chem.* **1992**, *31*, 3934.

(7) Balch, A. L.; Catalano, V. J. *Inorg. Chem.* **1991**, *31*, 2569.

(8) Balch, A. L.; Catalano, V. J. *Inorg. Chem.* **1991**, *30*, 1302.

(9) Balch, A. L.; Noll, B. C.; Olmstead, M. M.; Toronto, D. V. *Inorg. Chem.* **1992**, *31*, 5226.

0020-1669/93/1332-3613$04.00/0

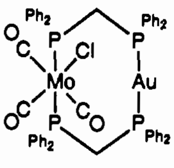

5

Mo-Au, 3.302 Å

(dpm-*P*)(CO)$_3$, which was the synthetic precursor that was used to form **5**,[9,10] with (t-BuNC)$_2$PdCl$_2$. We also undertook structural characterization of a previously reported d^6/d^8, Mo^0/Pd^{II} complex, MoPd(μ-dpm)$_2$(CO)$_3$(CN)$_2$, for which structure **A** had been proposed on the basis of spectroscopic data.[11] The presence of a Mo–Pd bond was discussed, and the possibility that one of the cyano groups might be bridging was also considered.[11] Structure **A** is particularly interesting because it implies a dative Pd→Mo bond in which a Pd^{II} center would donate electrons to an Mo^0 center. This direction of electron flow seems unusual since the more oxidized metal center would be acting as a donor. Consequently, further structural work on this compound was warranted.

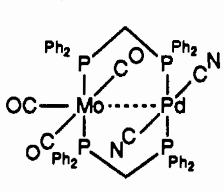

A

Results

Synthetic Studies. The reactions observed when *mer*-Mo(dpm-*P,P'*)(dpm-*P*)(CO)$_3$ is treated with (t-BuNC)$_2$PdCl$_2$ are dependent on the conditions that are utilized for the reaction. Scheme I summarizes our observations. When *mer*-Mo(dpm-*P,P'*)(dpm-*P*)(CO)$_3$ and (t-BuNC)$_2$PdCl$_2$ are mixed in dichloromethane, the solution turns red and then brown and finally stabilizes with a green color. When diethyl ether is mixed with the green solution, lime green crystals of [(t-BuNC)(OC)$_3$Mo(μ-dpm)$_2$PdCl]Cl (**6**) are obtained. The formation of **6** is accompanied by the formation of a second species which produces a pair of pseudotriplets of weaker integrated intensity in the ^{31}P NMR spectrum of the sample. Purification of **6** was not achieved, and its characterization relies on chemical transformations and spectroscopic data. Treatment of **6** with tri-*n*-butyl-*n*-propylammonium iodide and ammonium hexafluorophosphate produces a brown solution from which golden-brown crystals of [(t-BuNC)(OC)$_3$Mo(μ-dpm)$_2$PdI](PF$_6$) (**7**) are obtained by precipitation with ethyl ether.

Treatment of Mo(dpm-*P,P'*)(dpm-*P*)(CO)$_3$ with (t-BuNC)$_2$PdCl$_2$ in benzene produces a brown solution which remains brown and slowly deposits brown microcrystals of (t-BuNC)(OC)ClMo(μ-CO)(μ-dpm)$_2$PdCl (**8**). Addition of carbon monoxide to a brown solution of **8** in dichloromethane produces a lime green solution whose spectroscopic properties are consistent with the formation of **6**.

The ^{31}P{^{1}H} and ^{1}H NMR spectral data that characterize **6**–**8** are set out in Table I. The ^{31}P{^{1}H} NMR spectra of all three complexes follow a common pattern. Each consists of a pair of equally intense pseudotriplets. This pattern is consistent with the presence of the Mo(μ-dpm)$_2$Pd unit in each species. The ^{1}H NMR spectra indicate that a single *tert*-butyl isocyanide group is present in **7** and **8**. The methylene resonances of the dpm ligands in **6** and **7** show a single broad resonance, which suggests a locally symmetric arrangement of ligands about the Mo(μ-dpm)$_2$Pd unit. For these complexes, the methylene resonances do not appear to be sensitive to the asymmetric placement of the terminal carbon monoxide and *tert*-butyl isocyanide ligands on molybdenum. For **8**, two methylene resonances are observed. This is consistent with the A-frame-like nature of this complex, which has only a bridging carbon monoxide in addition to the dpm bridges.

Scheme I

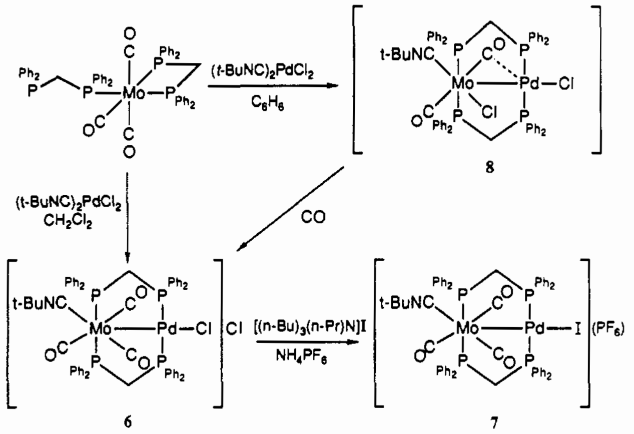

The infrared spectra of complexes **6**–**8** indicate that the isocyanide ligands reside in terminal positions: **6**, 2156 cm^{-1}; **7**, 2162 cm^{-1}; **8**, 2132 cm^{-1}. The infrared spectra for **6** and **7** show three carbon monoxide stretching bands: **6**, 2035, 1927, 1807 cm^{-1}; **7**, 2002, 1861, 1826 cm^{-1}. While these span a wide range, and the bands below 1900 cm^{-1} might easily be assigned to bridging carbon monoxide ligand, these data need to be viewed with caution. We previously showed that **5**, which has carbonyl stretching bands at 1952, 1830, and 1780 cm^{-1}, does not contain bridging carbon monoxide ligands.[9] The infrared spectrum of **8** shows only two carbon monoxide stretching vibrations: one at 1984 cm^{-1} and one at 1718 cm^{-1}. The latter is strongly suggestive of the presence of a bridging carbon monoxide of some sort.

Because the spectroscopic data are rather inconclusive in characterizing the arrangements of ligands within this closely related series of complexes, it was necessary to undertake X-ray crystallographic investigations of them. Fortunately **7** and **8** produce crystals of reasonable quality. Complex **6** was not obtained as suitable crystals, but the structure of **6** can easily be inferred from its chemical relationship to **7** and **8**.

Structure of [(t-BuNC)(OC)$_3$Mo(μ-dpm)$_2$PdI](PF$_6$)·0.5(C$_2$H$_5$)$_2$O·H$_2$O (7). Selected atomic coordinates are given in Table II, and important bond distances and angles are shown in Table III.

A view of the entire cation is shown in Figure 1. The cation has crystallographic mirror symmetry. Thus, the core that consists of the (CNC)(OC)Mo(CO)$_2$PdI unit is strictly planar.

The Mo–Pd distance (2.870(2) Å) in **7** is consistent with the existence of a single bond between these two atoms. Other distances for Mo–Pd single bonds span the range 2.723–3.060 Å (mean 2.811 Å) for the 28 examples in the Cambridge Crystallographic Data Base.[12] When the Mo–Pd bond is included, the molybdenum atom is seven-coordinate with a distorted pentagonal bipyramidal structure. The P(2)–Mo–P(2A) unit, with a bond angle of 175.8(1)°, forms the axial portion of this bipyramid. Within the equatorial plane, there is a wide deviation of the *cis*-bond angles from the ideal of 72°. The Pd–Mo–C(2) angle (53.4(4)°) is the narrowest while the C(1)–Mo–C(4) angle (86.9(5)°) is the widest. Alternately, the geometry about the molybdenum atom can be viewed in the context of a pseudooctahedral arrangement of ligands if the palladium atom is excluded.

---

(10) Blagg, A.; Shaw, B. L.; Thornton-Pett, M. *J. Chem. Soc., Dalton Trans.* **1987**, 769.

(11) Hassan, F. S. M.; Markham, D. P.; Pringle, P. G.; Shaw, B. L. *J. Chem. Soc., Dalton Trans.* **1985**, 279.

(12) Allen, F. H.; Kennard, O.; Taylor, R. *Acc. Chem. Res.* **1983**, *16*, 146.

Table I. NMR Spectral Data

	^{31}P{^{1}H} NMR^a			^{1}H NMR^a	
compound	$\delta(\mathrm{P_a})$, ppm	$\delta(\mathrm{P_B})$, ppm	N,^{b} Hz	$\delta(\mathrm{CH_2})$, ppm	$\delta(t\text{-Bu})$, ppm
[(t-BuNC)(OC)$_3$Mo(μ-dpm)$_2$PdCl]Cl, (**6**)	37.7	21.5	51.8	3.5	0.94
[(t-BuNC)(OC)$_3$Mo(μ-dpm)$_2$PdI](PF$_6$) (**7**)	35.7	8.7	48.6	3.6	0.91
(t-BuNC)(OC)ClMo(μ-CO)(μ-dpm)$_2$PdCl (**8**)	31.8	14.4	53.8	3.4, 3.9	0.75
(OC)$_3$(NC)Mo(μ-dpm)$_2$Pd(CN) (**9**)	38.0	19.7	48.7	4.1, 3.6	

^{a} Recorded in dichloromethane-d_2 at 25 °C. ^{b} $N = {}^2J(\mathrm{P_A,P_B}) + {}^4J(\mathrm{P_A,P_B})$.

Table II. Atomic Coordinates (×10^4) and Equivalent Isotropic Displacement Coefficients (Å^2 × 10^3) for [(t-BuNC)(OC)$_3$Mo(μ-dpm)$_2$PdI](PF$_6$)·0.5Et$_2$O·H$_2$O (**7**)^a

	x	y	z	U(eq)
Mo	7207(1)	7207(1)	3374(1)	23(1)*
Pd	7678(1)	7678(1)	2472(1)	23(1)*
I	8214(1)	8214(1)	1745(1)	31(1)*
P(1)	8422(1)	6974(1)	2435(1)	26(1)*
P(2)	7940(1)	6418(1)	3375(1)	27(1)*
N(1)	7169(5)	7169(5)	4585(4)	49(3)
O(1)	8189(3)	8189(3)	3511(4)	40(2)
O(2)	6780(3)	6780(3)	2326(3)	41(2)
O(3)	6240(3)	6240(3)	3614(5)	50(3)
C(1)	7835(4)	7835(4)	3426(4)	29(3)
C(2)	6984(4)	6984(4)	2695(5)	27(3)
C(3)	6577(5)	6577(5)	3519(5)	36(3)
C(4)	7197(4)	7197(4)	4166(5)	32(3)
C(5)	7115(8)	7115(8)	5135(5)	70(5)
C(6)	7350(7)	6563(8)	5289(4)	70(5)
C(7)	7655(9)	7655(9)	5304(7)	101(8)
C(20)	8222(4)	6288(4)	2747(3)	31(2)

^{a} An asterisk indicates the equivalent isotropic U defined as one-third of the trace of the orthogonalized U_{ij} tensor. Parameters for phenyl rings, hexaflouorophosphate, and ethyl ether are omitted. See supplementary material.

In that context, the C(1)–Mo–C(2) angle (115.4(5)°) is considerably widened from the 90° ideal and the C(2)–Mo–C(3) and C(3)–Mo–C(4) angles (79.5(5) and 78.2(5)°) are narrowed while the C(1)–Mo–C(4) angle (86.9(5)°) is near the ideal.

The palladium ion is four-coordinate with nearly planar geometry that involves the two *trans*-phosphine ligands, the iodide ligand, and the molybdenum atom.

Two of the carbonyl groups are in weakly semibridging positions. The Pd–C(1) and Pd–C(2) distances (2.627(12) and 2.318(12) Å) are much longer than the Mo–C(1) and Mo–C(2) distances (2.031(13) and 1.970(13) Å, respectively). Moreover, the Mo–C(1)–O(1) and Mo–C(2)–O(2) angles (172.7(11) and 168.0(10)°) show little bending. To some extent, the contacts between the palladium atom and these two carbon monoxide ligands are a simple consequence of the formation of the Mo–Pd bond. These two carbon monoxide ligands are unsymmetrically placed about the palladium ion, since the Pd–C(1) distance is considerably longer than the Pd–C(2) distance. The presence of linear semibridging carbonyl groups has previously been noted to result from crowded geometries where there was little or no direct bonding between the second metal and the carbon monoxide ligand on the first metal.[13,14]

Structure of (t-BuNC)(OC)ClMo(μ-CO)(μ-dpm)$_2$PdCl·2CHCl$_3$ (8). The asymmetric unit consists of one molecule of this complex and two chloroform molecules. Selected atomic coordinates are presented in Table IV, and Table V contains selected atomic distances and angles.

A view of the complex, which has no crystallographically imposed symmetry, is shown in Figure 2. The Mo–Pd distance (2.826(2) Å) is similar to the Mo–Pd distance seen in **7**. The overall geometry of **8** is related to that of **7**. The major differences involve the substitution of a terminal chloride for one of the semibridging carbon monoxide ligands in **7** and the reorientation of the other carbon monoxide so that it functions as a bridging group. These differences can be seen in Figure 3, which compares the planar inner cores of **7** and **8**.

In **8**, one carbon monoxide is oriented in an asymmetric bridging position between the two metals. While the two M–C distances (Mo–C(1) = 1.989(9), Pd–C(1) = 2.259(10) Å) are different, the Pd–C distance is clearly shorter than the Pd···C distances in **7**. Additionally the Mo–C(1)–O(1) angle (161.1(8)°) is more severely bent than are the Mo–C–O angles at the weakly semibridging groups in **7**.

The Mo–Cl distance (2.565(3) Å) lies within the range (2.335–2.618 Å, mean 2.446 Å) of 242 Mo–Cl distances in the Cambridge Crystallographic Data Base for compounds containing the MoP$_2$Cl structural entity.[12] This distance is shorter than the surprisingly long Mo–Cl bond (2.654(2) Å) found recently in the Au/Mo compound **5**.[9] The Pd···Cl distance is 3.106(1) Å, which is too long to represent a bonded interaction.

Structure of (OC)$_3$(NC)Mo(μ-dpm)$_2$Pd(CN)·CH$_3$OH·0.5H$_2$O (9). The complex (OC)$_3$(NC)Mo(μ-dpm)$_2$Pd(CN) (**9**) was obtained from the reaction of Pd(dpm-P,P')$_2$(CN)$_2$ with Mo(CO)$_3$(cyclohepta-1,3,5-triene) as reported previously.[11] It crystallizes with one molecule of **9**, one molecule of methanol, and one-half molecule of water in the asymmetric unit. Selected atomic coordinates are given in Table VI, and Table VII contains a list of important bond distances and angles.

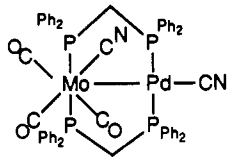

9

Figure 4 shows a view of the molecule. The overall structure follows the basic geometry that is present in **7** and **8**. Thus, there is a core *trans*-Mo(μ-dpm)$_2$Pd unit. The molybdenum center is bonded to an additional set of three terminal carbonyl groups and a cyanide ion. The other cyanide ion is bound as a terminal ligand on palladium. The Mo–Pd distance is 2.926(2) Å. This is longer than the corresponding distances in **7** and **8** as can be seen in Figure 3, but there are no immediately apparent causes for this lengthening.

In the structure of **9**, there is some question about the identities of the individual cyano and carbon monoxide ligands. The assignment of atoms shown in the figure gives the most satisfactory refinement as described in the Experimental Section.

Discussion

The reaction of *mer*-Mo(dpm-P,P')(dpm-P)(CO)$_3$ with (t-BuNC)$_2$PdCl$_2$ proceeds with opening of the strained, four-membered chelate ring and transfer of an isocyanide ligand to the open coordination site on molybdenum. The palladium is captured by the two free phosphorus atoms of the dpm ligands to form the (t-BuNC)(OC)$_3$Mo(μ-dpm)$_2$Pd unit. The complexes that are structurally characterized, **7** and **8**, have related geometries with very similar cores.

Both complexes (**7** and **8**) possess Mo–Pd single bonds. While the molybdenum geometry can be described in terms of a

---

[13] Crabtree, R. H.; Lavin, M. *Inorg. Chem.* **1986**, *25*, 805.
[14] Simpson, C. Q., II; Hall, M. B. *J. Am. Chem. Soc.* **1992**, *114*, 1641.

Table III. Bond Lengths (Å) and Angles (deg) for [(*t*-BuNC)(OC)$_3$Mo(μ-dpm)$_2$PdI](PF$_6$)·0.5Et$_2$O·H$_2$O (**7**)

	Bond Lengths		
Mo–Pd	2.870(2)	Mo–P(2)	2.457(2)
Mo–C(1)	2.031(13)	Mo–C(2)	1.970(13)
Mo–C(3)	2.073(15)	Mo–C(4)	2.142(13)
Mo–P(2A)	2.457(2)	Pd–I	2.619(1)
Pd–P(1)	2.340(2)	Pd–C(1)	2.627(12)
Pd–C(2)	2.318(12)	N(1)–C(5)	1.497(18)
N(1)–C(4)	1.133(18)	O(2)–C(2)	1.193(16)
O(1)–C(1)	1.166(16)		
O(3)–C(3)	1.116(18)		
	Bond Angles		
Pd–Mo–P(2)	91.2(1)	Pd–Mo–C(1)	62.1(3)
P(2)–Mo–C(1)	92.1(1)	Pd–Mo–C(2)	53.4(4)
P(2)–Mo–C(2)	89.3(1)	C(1)–Mo–C(2)	115.4(5)
Pd–Mo–C(3)	132.9(4)	P(2)–Mo–C(3)	87.9(1)
C(1)–Mo–C(3)	165.1(5)	C(2)–Mo–C(3)	79.5(5)
Pd–Mo–C(4)	149.0(4)	P(2)–Mo–C(4)	89.9(1)
C(1)–Mo–C(4)	86.9(5)	C(2)–Mo–C(4)	157.7(5)
C(3)–Mo–C(4)	78.2(5)	Pd–Mo–P(2A)	91.2(1)
P(2)–Mo–P(2A)	175.8(1)	C(1)–Mo–P(2A)	92.1(1)
C(2)–Mo–P(2A)	89.3(1)	C(3)–Mo–P(2A)	87.9(1)
C(4)–Mo–P(2A)	89.9(1)	Mo–Pd–I	170.5(1)
Mo–Pd–P(1)	92.9(1)	I–Pd–P(1)	87.1(1)
Mo–Pd–C(2)	43.1(3)	Mo–Pd–P(1A)	92.9(1)
P(1)–Pd–C(2)	92.1(1)	P(1)–Pd–P(1A)	174.1(1)
I–Pd–C(2)	146.5(3)	C(2)–Pd–P(1A)	92.2(1)
I–Pd–P(1A)	87.1(1)	C(4)–N(1)–C(5)	177.9(18)
Mo–C(2)–O(2)	168.0(10)	Mo–C(1)–O(1)	172.7(11)
Mo–C(3)–O(3)	177.6(13)	Pd–C(2)–O(2)	108.4(9)
P(1)–C(20)–P(2)	111.8(4)	Mo–C(4)–N(1)	176.3(13)

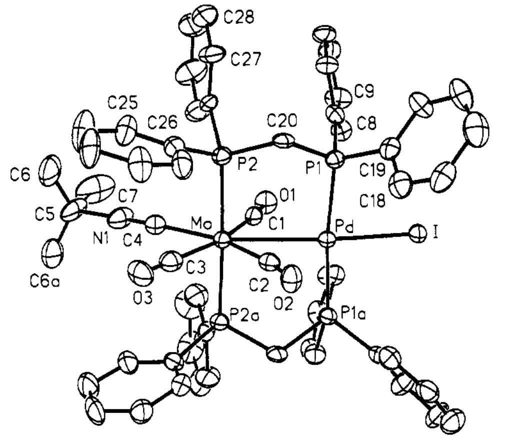

Figure 1. Perspective view of the monocation in [(*t*-BuNC)(OC)$_3$Mo(μ-dpm)$_2$PdI](PF$_6$) (**7**) with 50% thermal contours.

pentagonal bipyramid, it can be seen from the drawings that the arrangement of ligands is close to octahedral if the Mo–Pd bond is omitted. Thus, the bonding within the Mo(CNR)(CO)$_3$P$_2$ portion can be viewed as characteristic for a low-spin d^6 complex that conforms to the 18-electron rule. This leaves the filled, t$_{2g}$-like orbitals on molybdenum available for formation of the Mo–Pd bond. With the P–Mo–P axis as the *z* axis, the d$_{xy}$ orbital is available to act as a donor toward palladium and can form a donor/acceptor bond. The electron-poor P$_2$PdL$^+$ (L = Cl$^-$, I$^-$, CN$^-$) unit makes a suitable acceptor, and the dative Mo–Pd bond acts to complete planar coordination at palladium. Under this arrangement, the low-valent molybdenum acts as a donor to the more oxidized palladium center.

Table IV. Atomic Coordinates (×10^4) and Equivalent Isotropic Displacement Coefficients (Å^2 × 10^3) (*t*-BuNC)(OC)ClMo(μ-CO)(μ-dpm)$_2$PdCl·2CHCl$_3$ (**8**)[a]

	x	*y*	*z*	*U*(eq)
Mo	827(1)	1521(1)	1749(1)	15(1)*
Pd	1029(1)	2244(1)	807(1)	17(1)*
Cl(1)	2199(2)	2435(1)	2042(1)	24(1)*
Cl(2)	1447(2)	3078(1)	252(1)	27(1)*
N(1)	1114(8)	1444(4)	3107(3)	30(3)*
O(1)	−564(6)	1169(3)	570(3)	23(2)*
O(2)	−296(6)	220(3)	1780(3)	33(3)*
P(1)	2610(2)	959(1)	1700(1)	18(1)*
P(2)	2789(2)	1787(1)	728(1)	19(1)*
P(3)	−668(2)	2785(1)	810(1)	19(1)*
P(4)	−1015(2)	2054(1)	1811(1)	20(1)*
C(1)	49(9)	1381(4)	965(4)	21(3)*
C(2)	102(8)	706(5)	1771(4)	20(3)*
C(3)	1000(8)	1419(4)	2635(4)	20(3)*
C(4)	1216(10)	1559(5)	3703(4)	32(4)*
C(5)	2398(13)	1449(10)	3966(6)	162(13)*
C(6)	446(15)	1120(8)	3936(6)	110(9)*
C(7)	806(18)	2187(7)	3774(5)	139(12)*
C(20)	3585(8)	1418(4)	1355(4)	19(2)

[a] An asterisk indicates the equivalent isotropic *U* defined as one-third of the trace of the orthogonalized U$_{ij}$ tensor. Parameters for phenyl rings and chloroform are omitted. See supplementary material.

The structure of **9**, which is formed by a route that is distinct from that used for **7** and **8**, is closely related to those of **7** and **8** and is particularly similar to **7**. In both of these (**7** and **9**), the palladium center sits between two ligands: two carbonyl groups in **7**; a carbonyl group and a cyano group in **9**. These carbonyl and cyano ligands, however, maintain nearly linear Mo–C–O and Mo–C–N units. Thus, these very weakly semibridging groups interact only slightly with the palladium atom. This weak interaction is also reflected in the long Pd–C distances in **7** and **9**. In all cases, the Mo–Pd distances fall in the range expected for a Mo–Pd single bond. The occurrence of common structural features in **7**–**9** attests to the stability and importance of this basic structural unit in these d^6/d^8 complexes.

Of all of the compounds with Pd–Mo bonds, **7**–**9** appear most closely related to (OC)$_4$Mo(μ-PCy$_2$)$_2$Pd(PPh$_3$) (**10**).[15] This

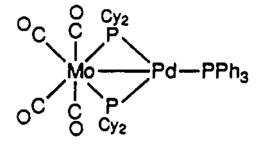

10

complex can be viewed as containing a six-coordinate molyb-

Table V. Bond Lengths (Å) and Angles (deg) for (t-BuNC)(OC)ClMo(μ-CO)(μ-dpm)$_2$PdCl (**8**)

	Bond Lengths		
Mo–Pd	2.826(2)	Mo–Cl(1)	2.565(3)
Mo–P(1)	2.453(3)	Mo–P(4)	2.491(3)
Mo–C(1)	1.989(9)	Mo–C(2)	1.956(10)
Mo–C(3)	2.148(10)	Pd–Cl(2)	2.356(3)
Pd–P(2)	2.341(3)	Pd–P(3)	2.321(3)
Pd–C(1)	2.259(10)	N(1)–C(3)	1.136(12)
N(1)–C(4)	1.460(13)	O(1)–C(1)	1.183(11)
O(2)–C(2)	1.149(12)		
	Bond Angles		
Pd–Mo–Cl(1)	70.2(1)	Pd–Mo–P(1)	91.5(1)
Cl(1)–Mo–P(1)	83.5(1)	Pd–Mo–P(4)	90.3(1)
Cl(1)–Mo–P(4)	98.4(1)	P(1)–Mo–P(4)	177.7(1)
Pd–Mo–C(1)	52.5(3)	Cl(1)–Mo–C(1)	122.7(3)
P(1)–Mo–C(1)	97.2(3)	P(4)–Mo–C(1)	82.9(3)
Pd–Mo–C(2)	128.3(3)	Cl(1)–Mo–C(2)	159.5(3)
P(1)–Mo–C(2)	86.8(3)	P(4)–Mo–C(2)	91.0(3)
C(1)–Mo–C(2)	76.4(4)	Pd–Mo–C(3)	150.6(3)
Cl(1)–Mo–C(3)	82.0(3)	P(1)–Mo–C(3)	94.5(3)
P(4)–Mo–C(3)	84.5(3)	C(1)–Mo–C(3)	153.7(4)
C(2)–Mo–C(3)	80.8(4)	Mo–Pd–Cl(2)	161.2(1)
Mo–Pd–P(2)	92.7(1)	Cl(2)–Pd–P(2)	89.3(1)
Mo–Pd–P(3)	93.9(1)	Cl(2)–Pd–P(3)	83.9(1)
P(2)–Pd–P(3)	173.2(1)	Mo–Pd–C(1)	44.3(2)
Mo–C(1)–O(1)	161.1(8)	Cl(2)–Pd–C(1)	153.3(2)
P(2)–Pd–C(1)	99.3(3)	P(3)–Pd–C(1)	86.6(3)
C(3)–N(1)–C(4)	172.6(10)	Mo–C(1)–Pd	83.1(3)
Mo–C(3)–N(1)	171.3(8)	P(1)–C(20)–P(2)	110.4(5)
P(3)–C(45)–P(4)	109.1(5)		

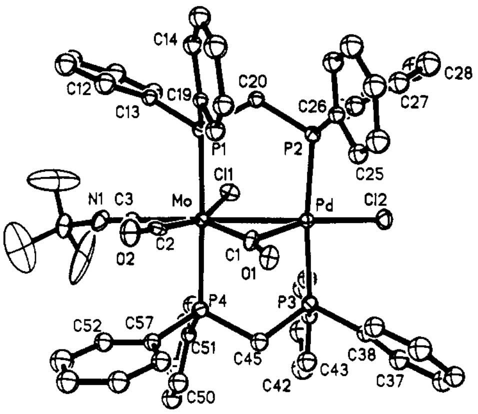

Figure 2. Perspective view of (t-BuNC)(OC)ClMo(μ-CO)(μ-dpm)$_2$PdCl (**8**) with 50% thermal contours.

denum(0) which also uses a pair of electrons in the d_{xy} orbital to form a dative Mo–Pd bond. However the Mo–Pd bond (2.760(1) Å) in **10** is shorter than that in the complexes reported here.

It is interesting to compare the geometry of **5**, which has no Mo–Au bond, to those of **7**–**9**, which do have Mo–Pd bonds. Thus, the P_2PdL^+ group is a better acceptor than the P_2Au^+ group. This is not unexpected. The higher oxidation state of the palladium certainly contributes to this. Additionally, there are numerous, two-coordinate complexes of gold(I) that are perfectly stable as 14-electron compounds. On the other hand, stable 14-electron complexes of the type L_3Pd^{II} are virtually unknown. It is also interesting that in **8** it is the molybdenum rather than the molybdenum-bonded chloro ligand that supplies the additional two electrons to palladium.

Experimental Section

Preparation of Compounds. (t-BuNC)$_2$PdCl$_2$,[16] *mer*-Mo(dpm-*P*,*P*′)(dpm-*P*)(CO)$_3$,[17] and **9**[11] were prepared by standard routes. The new compounds described here are stable to moisture and dioxygen and can be prepared without recourse to inert-atmosphere techniques.

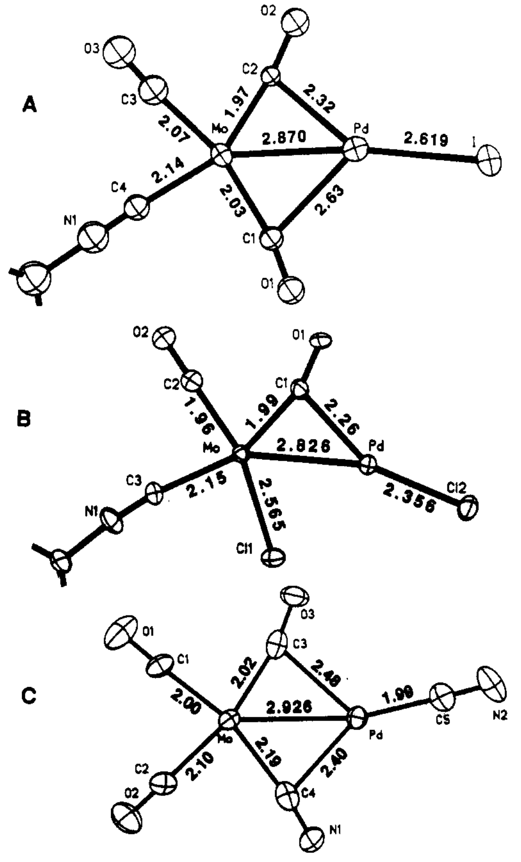

Figure 3. Comparison of dimensions within the planar or nearly planar cores of (A) [(t-BuNC)(OC)$_3$Mo(μ-dpm)$_2$PdI](PF$_6$) (**7**), (B) (t-BuNC)(OC)ClMo(μ-CO)(μ-dpm)$_2$PdCl (**8**), and (C) (OC)$_3$(NC)Mo(μ-dpm)$_2$Pd(CN) (**9**).

[(t-BuNC)(OC)$_3$Mo(μ-dpm)$_2$PdCl]Cl (6). To 100 mg (0.106 mmol) of *mer*-Mo(dpm-*P*,*P*′)(dpm-*P*)(CO)$_3$ dissolved in 20 mL of dichloromethane was added 40 mg (0.114 mmol) of (t-BuNC)$_2$PdCl$_2$. Within a period of 10 min, the solution turned red, then brown, and finally green. After 20 min of stirring, the volume was reduced to 10 mL and addition of diethyl ether resulted in a lime-green solid. Complete purification was not achieved. A second species with ^{31}P NMR resonances at δ_1 = 36.1

---

(15) Loeb, S. J.; Taylor, H. A.; Gelmini, L.; Stephan, D. W. *Inorg. Chem.* **1986**, *25*, 1977.

(16) Crociano, B.; Boschi, T.; Belluco, U. *Inorg. Chem.* **1970**, *9*, 2021.

(17) Graham, W. A. G.; Isaacs, E. E. *Inorg. Chem.* **1975**, *14*, 2560.

Table VI. Atomic Coordinates ($\times 10^4$) and Equivalent Isotropic Displacement Coefficients ($Å^2 \times 10^3$) for $(OC)_3(NC)Mo(\mu\text{-dpm})_2Pd(CN)\cdot CH_3OH\cdot 0.5H_2O$ (**9**)[a]

	x	*y*	*z*	*U*(eq)
Pd	2565(1)	1111(1)	2671(1)	26(1)
Mo	1293(1)	2715(1)	3524(1)	25(1)
P(1)	1762(3)	3342(3)	2450(3)	29(2)
P(2)	3092(2)	1669(3)	1651(3)	29(2)
P(3)	2096(3)	365(3)	3573(3)	30(2)
P(4)	608(3)	1933(3)	4408(3)	28(2)
O(1)	1551(12)	4894(9)	5197(9)	64(7)
O(2)	−1161(9)	3107(9)	3139(8)	47(6)
O(3)	3738(8)	2981(8)	4463(7)	39(5)
N(1)	274(11)	540(10)	1722(10)	40(6)
N(2)	4350(11)	−268(12)	2165(11)	50(8)
C(1)	1430(12)	4084(11)	4575(11)	34(8)
C(2)	−298(11)	2965(11)	3258(11)	29(7)
C(4)	693(12)	1261(13)	2329(11)	33(8)
C(3)	2863(12)	2786(11)	4036(11)	32(7)
C(5)	3697(12)	230(12)	2327(11)	35(8)
C(7)	3555(8)	4753(8)	3667(7)	44(4)

[a] *U*(eq) is the equivalent isotropic *U* defined as one-third the trace of the orthogonalized U_{ij} tensor. Parameters for phenyl rings and solvate atoms are omitted. See supplementary material.

ppm and δ_2 = 19.8 ppm (pseudotriplets) was present and could not be removed by recrystallization (yield 40%).

[(*t*-BuNC)(OC)$_3$Mo(μ-dpm)$_2$PdI](PF$_6$) (7). Method I. A 100-mg (0.281-mmol) portion of tri-*n*-butyl-*n*-propylammonium iodide was added to the green solution formed in the synthesis of **6**. After the solution turned brown, it was stirred for 30 min. Then, 18 mg (0.11 mmol) of ammonium hexafluorophosphate in 20 mL of methanol was added. The solution was stirred for 15 min, after which the volume was reduced under vacuum to 10 mL. Addition of diethyl ether afforded golden-brown crystals which were collected by filtration and recrystallized from dichloromethane and diethyl ether (yield 84%).

Method II. To 80 mg (0.053 mmol) of **6** in dichloromethane was added 40 mg (0.106 mmol) of tri-*n*-butyl-*n*-propylammonium iodide. The green solution immediately turned brown. A solution of 18 mg (0.11 mmol) of ammonium hexafluorophosphate in 20 mL of methanol was added. After 2 h of stirring, the volume was reduced to 10 mL. Diethyl ether was added to precipitate the golden-brown product from the filtrate (yield 55%).

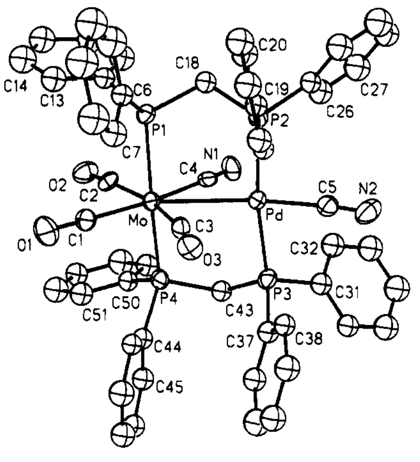

Figure 4. Perspective view of $(OC)_3(NC)Mo(\mu\text{-dpm})_2Pd(CN)$ (**9**) with 50% thermal contours.

(*t*-BuNC)(OC)ClMo(μ-CO)(μ-dpm)$_2$PdCl (8). To 100 mg (0.106 mmol) of *mer*-Mo(dpm-*P,P'*)(dpm-*P*)(CO)$_3$ in 40 mL of benzene was added 40 mg (0.114 mmol) of (t-BuNC)$_2$PdCl$_2$. The solution turned immediately brown and was stirred for 60 min. At this time, brown microcrystals started to form. The product was collected by filtration and washed with diethyl ether (yield 73%).

Physical Measurements. The $^{31}P\{^1H\}$ NMR spectra were recorded on a General Electric QE-300 NMR spectrometer operating at 121.7 MHz with an external 85% phosphoric acid standard and the high-field positive convention for chemical shifts. Infrared measurements were recorded for hydrocarbon mulls on an IBM 32 spectrometer.

X-ray Data Collection. [(*t*-BuNC)(OC)$_3$Mo(μ-dpm)$_2$PdI](PF$_6$)·0.5Et$_2$O·H$_2$O (7). Orange-brown plates were obtained by diffusion of diethyl ether into a chloroform solution of the complex. A single crystal was mounted on a glass fiber with silicone grease and placed in the 130 K nitrogen stream of a Siemens R3m/V diffractometer with a modified

Table VII. Bond Lengths (Å) and Angles (deg) for $(OC)_3(NC)Mo(\mu\text{-dpm})_2Pd(CN)\cdot CH_3OH\cdot 0.5H_2O$ (**9**)

	Bond Lengths		
Pd–Mo	2.926(2)	Pd–P(2)	2.327(6)
Pd–P(3)	2.332(6)	Pd–C(4)	2.402(16)
Pd–C(3)	2.482(13)	Pd–C(5)	1.989(16)
Mo–P(1)	2.459(6)	Mo–P(4)	2.433(6)
Mo–C(1)	1.995(13)	Mo–C(2)	2.096(15)
Mo–C(4)	2.185(14)	Mo–C(3)	2.022(16)
O(1)–C(1)	1.177(17)	O(2)–C(2)	1.133(19)
O(3)–C(3)	1.167(18)	N(1)–C(4)	1.126(17)
N(2)–C(5)	1.14(2)	N(1)–C(4)	1.126(17)
	Bond Angles		
Mo–Pd–P(2)	93.7(1)	Mo–Pd–P(3)	93.0(1)
P(2)–Pd–P(3)	172.9(1)	Mo–Pd–C(4)	47.2(3)
P(2)–Pd–C(4)	92.2(5)	P(3)–Pd–C(4)	90.7(5)
Mo–Pd–C(3)	42.9(4)	P(2)–Pd–C(3)	95.9(5)
P(3)–Pd–C(3)	90.5(5)	C(4)–Pd–C(3)	90.0(5)
Mo–Pd–C(5)	167.0(4)	P(2)–Pd–C(5)	87.3(6)
P(3)–Pd–C(5)	86.7(6)	C(4)–Pd–C(5)	145.8(5)
C(3)–Pd–C(5)	124.0(5)	Pd–Mo–P(1)	88.9(1)
Pd–Mo–P(4)	90.5(1)	P(1)–Mo–P(4)	171.6(1)
Pd–Mo–C(1)	141.3(5)	P(1)–Mo–C(1)	93.2(6)
P(4)–Mo–C(1)	92.5(6)	Pd–Mo–C(2)	136.5(3)
P(1)–Mo–C(2)	86.9(5)	P(4)–Mo–C(2)	87.8(5)
C(1)–Mo–C(2)	82.2(6)	Pd–Mo–C(4)	53.7(4)
P(1)–Mo–C(4)	87.8(6)	P(4)–Mo–C(4)	85.0(6)
C(1)–Mo–C(4)	164.9(6)	C(2)–Mo–C(4)	82.8(6)
Pd–Mo–C(3)	56.7(4)	P(1)–Mo–C(3)	94.5(6)
P(4)–Mo–C(3)	92.2(6)	C(1)–Mo–C(3)	84.6(6)
C(2)–Mo–C(3)	166.8(5)	C(4)–Mo–C(3)	110.4(6)
Mo–C(1)–O(1)	177.6(14)	Mo–C(2)–O(2)	178.0(15)
Pd–C(4)–Mo	79.1(4)	Pd–C(4)–N(1)	108.3(13)
Mo–C(4)–N(1)	172.5(15)	Pd–C(3)–Mo	80.3(4)
Pd–C(3)–O(3)	111.7(11)	Mo–C(3)–O(3)	167.8(12)
Pd–C(5)–N(2)	177.3(17)		

Table VIII. Crystallographic Data for [(*t*-BuNC)$(OC)_3$Mo(μ-dpm)$_2$PdI](PF_6)·0.5Et_2O·H_2O (**7**), (*t*-BuNC)(CO)ClMo(μ-CO)(μ-dpm)PdCl·2$CHCl_3$ (**8**), and $(OC)_3$(NC)Mo(μ-dpm)$_2$Pd(CN)·CH_3OH·0.5H_2O (**9**)

	7	**8**	**9**
chem formula	$C_{60}H_{60}F_6IMoNO_{4.5}P_5Pd$	$C_{59}H_{55}Cl_8MoNO_2P_4Pd$	$C_{56}H_{48}MoN_2O_{4.5}P_4Pd$
crystal system	tetragonal	monoclinic	triclinic
space group	$I\bar{4}2m$	$P2_1/c$	$P\bar{1}$
a, Å	22.822(4)	11.825(6)	12.486(3)
b, Å		21.508(12)	15.213(6)
c, Å	27.013(7)	24.441(13)	16.511(7)
α, deg			116.85(2)
β, deg		100.77(4)	96.17(2)
γ, deg			95.40(2)
V, Å^3	14 070(5)	6107(6)	
Z	8	4	2
fw	1438.1	1419.9	1147.2
T, K	130	130	130
λ(Mo Kα), Å	0.710 73	0.710 73	0.710 73
μ(Mo Kα), cm^{-1}	10.43	9.97	7.18
d_{calc}, Mg/m^3	1.383	1.544	1.388
$R(F_o)^a$	0.049	0.069	0.083
$R_w(F_o)^b$	0.053	0.061	0.089
transm factors	0.65–0.86	0.83–0.90	0.71–0.97

[a] $R = \sum||F_o| - |F_c||/\sum||F_o|$. [b] $R_w = \sum||F_o| - |F_c||w^{1/2}/\sum|F_o|w^{1/2}$.

Enraf-Nonius low-temperature apparatus. Two check reflections showed only random fluctuations (<2%) in intensity throughout the data collection. The data were corrected for Lorentz and polarization effects. Crystal data are given in Table VIII.

(*t*-BuNC)(OC)ClMo(μ-CO)(μ-dpm)$_2$PdCl·2$CHCl_3$ (8). Red-brown blocks were obtained by diffusion of diethyl ether into a benzene solution of the complex. The crystal was mounted as described above in the cold stream of a Syntex P2$_1$ diffractometer that was fitted with a modified LT-1 low-temperature device. Two check reflections showed only random (<2%) fluctuations in intensity during data collection. The data were corrected for Lorentz and polarization effects.

$(OC)_3$(NC)Mo(μ-dpm)$_2$Pd(CN)·CH_3OH·0.5H_2O (9). Brown-green plates were obtained by slow diffusion of diethyl ether into a dichloromethane solution of the complex. The crystal was mounted as described above for **7**.

Structure Solution and Refinement. [(*t*-BuNC)$(OC)_3$Mo(μ-dpm)$_2$PdI](PF_6)·0.5Et_2O·H_2O (7). Calculations were performed using SHELXTL PLUS (PC and VMS versions) software. Scattering factors and corrections for anomalous dispersion were taken from a standard source.[18] An absorption correction was applied.[19] The structure was solved by Patterson techniques. There are eight cations in the unit cell. Each is bisected by a mirror plane that passes through the atoms Mo, Pd, I, C(1)–C(5), C(7), O(1)–O(3), and N(1). Within the unit cell there are two sites for hexafluorophosphate anions. One has S_4 symmetry, is fully occupied, and accounts for four anions. The other is bisected by a mirror plane, has 0.5 fractional occupancy, and accounts for four anions within the unit cell. There is a diethyl ether molecule at fractional occupancy which also occupies the space at the site when the hexafluorophosphate is absent. Another diethyl ether molecule is present at fractional occupancy at a separate site. Three regions of electron density have been modeled as water molecules at fractional occupancy. Mo, Pd, I, P(1)–P(3), N(1), C(1)–C(32), O(1)–O(3), and two fluorine atoms of one hexafluorophosphate were refined with anisotropic thermal parameters. The largest peak (1.12 e/Å^3) in the final difference map was located between the fluorine atoms of a hexafluorophosphate ion.

(*t*-BuNC)(OC)ClMo(μ-CO)(μ-dpm)$_2$PdCl·2$CHCl_3$ (8). The structure was solved and refined as described above except that anisotropic thermal parameters were refined for Mo, Pd, Cl, P, N, and O and the carbons of the carbonyl and isocyanide groups. Some elongation of the thermal ellipsoids of the *tert*-butyl group is observed. This is likely to be due to the rotational disorder about the C(4)–N(1) bond. The largest peak (1.62 e/Å^3) in the final difference map is 1.46 Å from C(7) and is probably due to disorder of the *tert*-butyl group.

$(OC)_3$(NC)Mo(μ-dpm)$_2$Pd(CN)·CH_3OH·0.5H_2O (9). The structure was solved by Patterson methods and refined as described for **7**. Anisotropic thermal parameters were assigned to the palladium, molybdenum, and phosphorus atoms and the carbon, nitrogen, and oxygen atoms of the carbonyl and cyanide ligands. During initial refinement, the terminal atoms attached to C(1) through C(5) were treated as oxygen atoms (*i.e.*, the cyano groups were treated as carbon monoxide ligands). Subsequently, the thermal parameters for the atoms now identified as N(1) and N(2) were found to be larger than those of O(1)–O(3). On this basis, these atoms were treated as nitrogen atoms. This assignment then gave thermal parameters of size comparable to those of all the terminal atoms of the carbon monoxide and cyano ligands. A variety of alternative assignments were considered; all gave a wider range of thermal parameters for the presumed oxygen and nitrogen atoms. All phenyl rings were modeled with idealized geometry. Hydrogen atoms were fixed at calculated positions through the use of a riding model in which the C–H vector was fixed at 0.96 Å and the isotropic thermal parameter for each hydrogen was fixed at 0.036 Å^2. The largest peak (1.62 e/Å^3) in the final difference map was 0.92 Å from the palladium atom.

Acknowledgment. We thank the National Science Foundation (Grant CHE 9022909) for support, Johnson Matthey Inc. for a loan of palladium, and Prof. V. J. Catalano for helpful discussions.

Supplementary Material Available: Tables of atomic coordinates, bond distances, bond angles, anisotropic thermal parameters, hydrogen atom positions, and crystal data for **7**–**9** (28 pages). Ordering information is given on any current masthead page.

---

(18) *International Tables for X-ray Crystallography*; Kynock Press: Birmingham, England, 1974; Vol. 4.

(19) The method obtains an empirical absorption tensor from an expression relating F_o and F_c: Moezzi, B. Ph.D. Thesis, University of California, Davis, 1987.